DOI: 10.18727/0722-6691/5019

The Adaptive Optics Facility: Commissioning Progress and Results

Robin Arsenault[1]
Pierre-Yves Madec[1]
Elise Vernet[1]
Wolfgang Hackenberg[1]
Paolo La Penna[1]
Jérome Paufique[1]
Harald Kuntschner[1]
Jean-François Pirard[1]
Johann Kolb[1]
Norbert Hubin[1]

[1] ESO

All the Adaptive Optics Facility (AOF) subsystems are now in Paranal and the project team is working on commissioning activities on Unit Telescope 4 (UT4) of the Very Large Telescope. Excellent progress has been made; the new secondary mirror unit, the Deformable Secondary Mirror (DSM), was installed in October 2016 and UT4 is now operating routinely with the DSM in non-adaptive optics mode. The other modules of the AOF, the Ground Atmospheric Layer Adaptive optiCs for Spectroscopic Imaging (GALACSI), the 4 Laser Guide Star Facility (4LGSF) and the GRound-layer Adaptive optics Assisted by Lasers (GRAAL), have been installed and are being qualified. The coupling with the High Acuity Wide field *K*-band Imager (HAWK-I) and the Multi Unit Spectroscopic Explorer (MUSE) has been tested and all elements are functional and ready to proceed with their full commissioning. The goal for the AOF is to complete GALACSI wide-field mode technical commissioning by the end of summer 2017 and the GRAAL ground-layer adaptive optics mode by the end of the year.

ESO Project Team:

D. Bonaccini Calia, P. Duhoux, J.-L. Lizon, S. Guisard, P. Lilley, L. Petazzi, P. Hammersley, I. Guidolin, L. Kern, T. Pfrommer, C. Dupuy, R. Guzman, J. Quentin, M. Quattri, R. Hozlöhner, D. Popovic, M. Comin, S. McClay, S. Lewis, F. Gago, M. Sarazin, P. Haguenauer, A. Jost, J. Argomedo, S. Tordo, R. Donaldson, R. Conzelmann, M. Lelouarn, R. Siebenmorgen, M. Downing, J. Reyes, M. Suarez Valles, S. Stroebele, S. Oberti, P. Gutierrez Cheetam, M. Kiekebusch, C. Soenke, E. Aller-Carpentier, P. Jolley, J. Vernet, A. Manescau-Hernandez, L. Mehrgan, G. Calderone, A. van Kesteren, G. Chiozzi, H. Sommers, D. Dorigo, T. Bierwirth, J.-P. Kirchbauer, S. Huber, G. Fischer, A. Haimerl, S. Leveque, P. Amico, G. Hubert, S. Brillant, P. Baksai, J.C. Palacio, I. Munoz, E. Fuenteseca, P. Bourget, P. Hibon, F. Selman, G. Hau, S. Egner, T. Szeifert, J.C. Guerra.

Introduction

Towards the end of 2016, the only missing pieces of the Adaptive Optics Facility (AOF) complex (see Arsenault et al., 2010, 2014a and 2016 for previous progress updates) were the new secondary mirror (M2) unit — the Deformable Secondary Mirror (DSM) — and the Ground Atmospheric Layer Adaptive optiCs for Spectroscopic Imaging (GALACSI) adaptive optics (AO) module. The new M2 unit was installed in October 2016 during a shutdown of Unit Telescope 4 (UT4 — Yepun) and the whole telescope was recommissioned with the new M2 unit by December 2016. Since then, UT4 has returned to operations and the Paranal telescope and instrument operators (TIOs) and science support staff have been trained to use the telescope with this new secondary mirror in non-adaptive optics mode. The AOF team remains in close contact with Paranal staff and closely monitors any errors and issues to provide support and solutions.

At the end of 2016, the GALACSI instrument was dismounted from the Adaptive Secondary Simulator and InStrument Testbed (ASSIST) in the Garching integration hall and packed for transport to Chile. After reintegration in Paranal, all functionalities were recovered. In late March 2017, GALACSI was installed on UT4 and was then ready to enter the commissioning phase.

The project is now fully involved in commissioning activities and these will continue during 2017 and into part of 2018. Commissioning runs are scheduled almost every month during bright time. Some of them may be returned to science operations if commissioning progress is rapid and if there are no technical problems or bad weather. The intention is to complete the commissioning of the Multi Unit Spectroscopic Explorer (MUSE) with the GALACSI Wide Field Mode (WFM) at the end of the summer 2017, with Science Verification planned for August 2017. Commissioning of the High Acuity Wide field *K*-band Imager (HAWK-I) and the GRound-layer Adaptive optics Assisted by Lasers (GRAAL) in ground layer adaptive optics (GLAO) mode is planned by the end of 2017. Then only MUSE with GALACSI in Narrow Field Mode (NFM) will remain to be commissioned in 2018.

Installation of new M2 unit on UT4

In September 2016, the 14 crates containing the DSM system (Arsenault et al., 2013a; Manetti et al., 2014; Briguglio et al., 2014), totalling 9 tonnes and 50 cubic metres, were unpacked in the New Integration Hall (NIH) in Paranal. The system was re-assembled in the NIH and functionalities tested. It was an opportunity to cross-train our Paranal colleagues and demonstrate several handling operations, including the critical thin-shell mirror handling.

Before proceeding with the removal of the old Dornier M2 unit, a laser tracker was installed on the telescope centrepiece and used to record reference positions of markers on the telescope structure and the M2 hub and spiders. Additionally, reference measurements were taken to characterise the telescope optical behaviour and performance, some of them using the GRAAL Maintenance and Commissioning Mode (MCM) wavefront sensor. Close-out measurements were also taken for the instruments available at UT4 (the Spectrograph for INtegral Field Observations in the Near Infrared [SINFONI], HAWK-I, MUSE and the VLT Interferometer [VLTI]) with the support of Science Operation. These would later be used to verify that telescope and instrument performance had not been degraded after the installation of the new M2 unit.

On 14 October 2016, the first transport took place to UT4 and the DSM hub was brought to the telescope. The next day the DSM followed the same route. Extreme care was taken during the transport and the load was accompanied on foot all the way to monitor the smoothness of the ride. The replacement began with the removal of the Beryllium M2 mirror. Then within one day the Dornier hub was removed and the new M2 hub, with its DSM dummy weight, installed instead. Three days later the DSM was installed in

Figure 1. A jubilant team after the installation of the DSM on UT4.

its hub (see p. 7). Using the laser tracker, it was possible to verify that the DSM hub ended up, after its installation on the telescope, within 1 mm of the Dornier hub's position, while its longitudinal axis was colinear within 1 arcminute. Calibrated mechanical spacers and alignment tools allowed this feat, as well as the expertise of the optical engineers in Garching and Paranal. The whole operation was led by the Paranal mechanical team under the close supervision of the contractor Microgate and the Garching DSM team.

It is amazing to think that, after such an intrusive and major operation on the telescope, the first pointing on sky was successful, with pointing errors of the same magnitude as usual, and the active loop was closed successfully after the first iteration! Figure 1 illustrates the effect of this achievement on the whole team.

Telescope re-commissioning

During the first nights after installation, basic tests were carried out to verify the behaviour of the DSM hexapod. The focusing motion was as expected and the three focal planes could be accommodated within the DSM focusing range. The impact of M2 centring on the telescope coma was measured using the GRAAL MCM wavefront sensor. Excellent agreement between the centring of the old Dornier and the new M2 was achieved, and the GRAAL MCM mode proved extremely useful during all the telescope recommissioning phases. It also shows that mechanical flexure introduced by the new M2 unit is fully comparable to that experienced with the old Dornier.

The new magnitude zero points for HAWK-I were found to be identical, within 3 %, to the former values and the emissivity was measured as 25 % for the Dornier and 24 % for the new M2 unit. The plate scale change was measured at 1.00047 ± 0.0005 on the Nasmyth B guide probe, which compares to 1.00067 when measured directly on HAWK-I; these results mean that, for all practical purposes, the plate scale change is negligible.

A series of 10-second *J*-band images were taken of the globular cluster M30 using the new M2 unit. Figure 2 (left) shows one of the best images obtained with the DSM, with a full width at half maximum (FWHM) of the star images of 0.37 arcseconds (visual band seeing was 0.5 arcseconds at the time of the exposure); see Figure 2, right. This measurement demonstrates that the optical quality of the DSM in non-adaptive optics mode allows seeing-limited observation even under excellent seeing conditions.

The next step consisted of assessing the changes in the operation of the active optics. The strategy was to record the active optics aberration measurements of the telescope after application of the so-called "OneCal", the look-up table for the primary mirror (M1) modes versus altitude. Comparisons were made between the Dornier and the DSM. The values are very similar between both, and the active optics functionality and operational aspects are preserved with the DSM as well. The secondary chopping was also tested and behaved as expected. Only two points remained to be examined — the flexure of the DSM reference body and the DSM flattening vector.

The trefoil and astigmatism terms evolve with altitude as can be seen in Figure 3. Only the terms along the altitude axis show a variation. This does not come as a surprise as it was known that the reference body of the DSM is subjected to this sort of deformation. At the zenith, the reference body is deformed in a threefold sag shape (trefoil) because of the system of three supporting points. At the horizon this deformation evolves toward an astigmatism. The left plot in Figure 3 shows that this variation is seen by the active optics of the telescope and corrected by M1. However, the level is quite acceptable and, since the end of the commissioning,

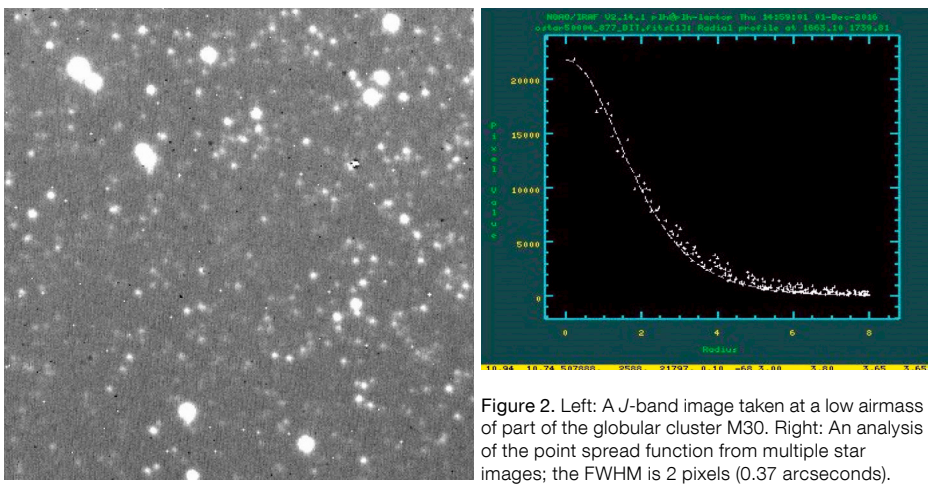

Figure 2. Left: A *J*-band image taken at a low airmass of part of the globular cluster M30. Right: An analysis of the point spread function from multiple star images; the FWHM is 2 pixels (0.37 arcseconds).

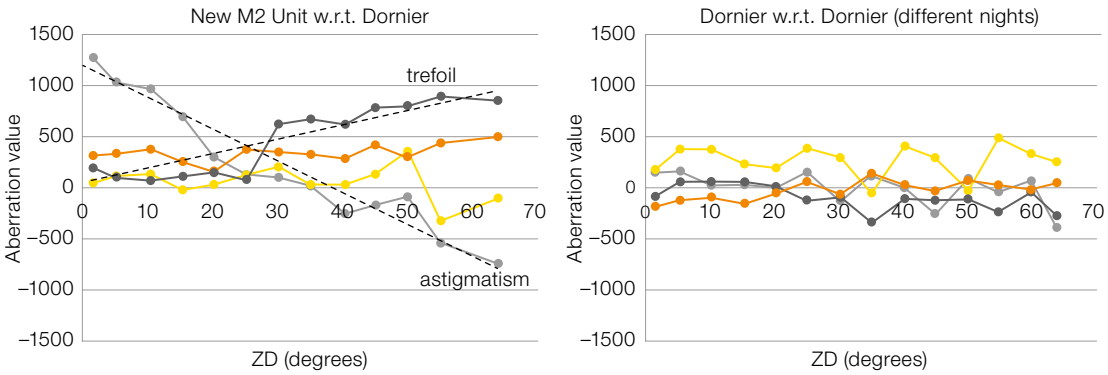

Figure 3. Left: The difference in OneCal residual aberrations between the DSM and the old Dornier M2 unit as a function of zenith distance (ZD). Zernike pairs of orthogonal modes for trefoil and astigmatism are shown. Right: Same as left figure but for two different sets of measurements of the Dornier M2 unit on different nights, showing the typical noise level. The DSM shows clear trends of the astigmatism and trefoil aberrations with altitude (zenith distance).

the active optics has managed this change without issue. Note that the corresponding mode amplitude applied in the DSM flattening vector has been modified to ensure that the horizontal axis crossover occurs at a typical operation airmass.

The same type of analysis reflected a slightly higher scatter in the higher M1 mode amplitudes. We believe that this is due to some high-order aberrations in the DSM flattening vector. After these measurements a calibration was carried out to optimise the DSM flattening vector and reduce its content in high-order aberrations.

Finally, a detailed analysis of the field stabilisation performance took place. Many small issues were encountered, resulting from the telescope environment and the somewhat different control parameters required by the DSM, but all were progressively resolved. The final performance is certainly adequate. The only remaining issue is poorer performance when the telescope is facing into a strong wind. More data need to be recorded to fully understand the root cause of this problem before it can be fixed.

An analysis of the field stabilisation closed-loop rejection transfer function was performed. For a control frequency of 32 Hz, integration time of 0.01 s and control parameters of K_p = 0.7, K_i = 1.5 and $K_{offload}$ = 0.02 and a 3 Hz cutoff frequency, a 6 dB overshoot (> 45° phase margin) was observed.

HD 49798	Before	After
K	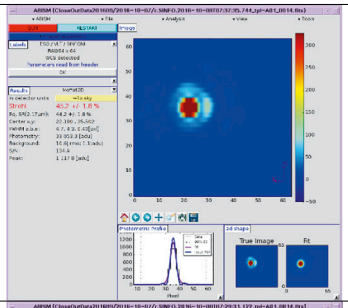	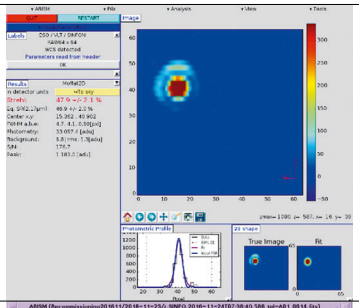
H+K	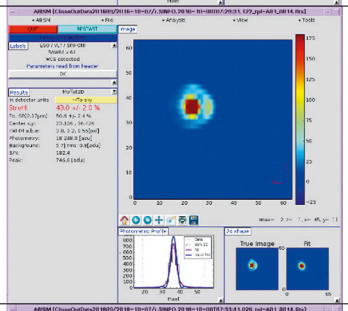	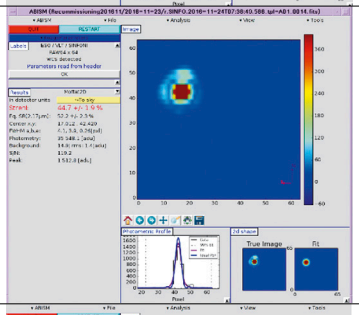
H	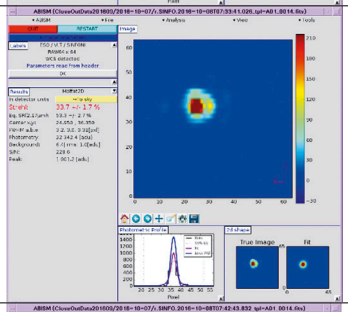	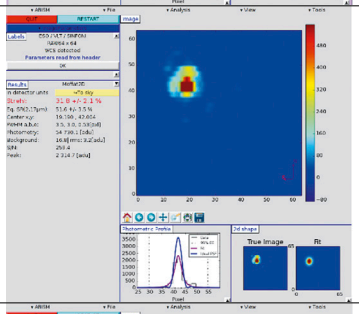
J	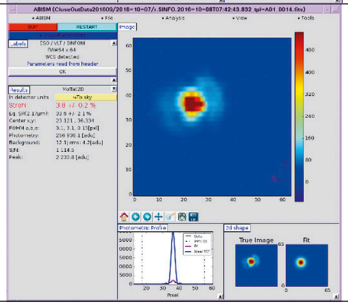	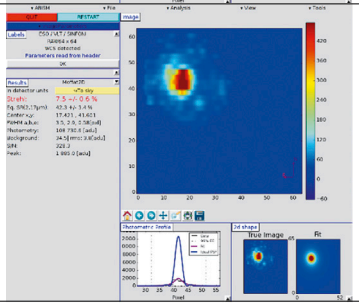

Figure 4. PSF samples for the star HD 49798. The "Before" and "After" columns refer to images obtained with the Dornier M2 unit and the new DSM M2 unit, respectively. The external seeing values were similar in both cases.

UT4 instrument recommissioning

To complete the recommissioning process, the instrument scientists of HAWK-I, MUSE, SINFONI and the VLTI performed a dedicated set of tests to assess the behaviour of these instruments after the new M2 installation. These tests addressed several aspects of the instruments' performance; we show here only a few excerpts from the recommissioning reports. Figure 4 shows a sample of SINFONI PSFs and corresponding Strehl ratios in different bands for the star HD 49798. The results are essentially identical, except in the *J*-band where high spatial frequency residuals can be noticed (static speckles around the diffraction limited core); these residuals are due to the high spatial frequency aberrations of the DSM optical surface. The situation was later improved by calibrating and updating the reference vector position of the DSM when in non-AO mode.

The HAWK-I recommissioning report also thoroughly reviewed several performance criteria for the instrument. The Two Micron All Sky Survey (2MASS) Touchstone Fields were observed and reduced using the new Cambridge Astronomy Survey Unit (CASU) pipeline. The variation of the FWHM across the whole field of view was compared and appeared as expected (see Figure 5). The ellipticity of the star images was also examined in the different fields. The report concluded that the installation of the new M2 unit has had no impact on the overall performance of HAWK-I.

The reports on MUSE and VLTI also concluded that the behaviour remained similar before and after the installation of the new M2 unit. Small differences were observed in behaviour, enough to realise that the M2 has been exchanged, but there was certainly no loss in performance with respect to the Dornier M2 unit.

DSM commissioning with the GRAAL Maintenance and Commissioning Mode

The last step of the new M2 commissioning was the verification of the performance of the DSM in AO mode. The GRAAL MCM mode (Arsenault et al., 2014b; Paufique et al., 2012) was developed for this purpose; it is based on single conjugate AO, making use of a 1 kHz – 40 × 40 subaperture wavefront sensor (WFS) looking at a bright natural guide star on-axis, therefore fully exploiting the 1172 actuators of the DSM. The tests were carried out during a run in February 2017. Unfortunately, many nights were lost to high humidity and only slightly more than half of the ten nights could be used for on-sky tests. The result is that less time was available to optimise the performance. In particular, not enough time was available to characterise the non-common path aberrations and apply an accurate offset for them on the DSM. Nevertheless, excellent images and performance could be obtained and all the servo-loops and offloads could be validated in this technical mode (this is, however, not a science observing mode; see Figure 6).

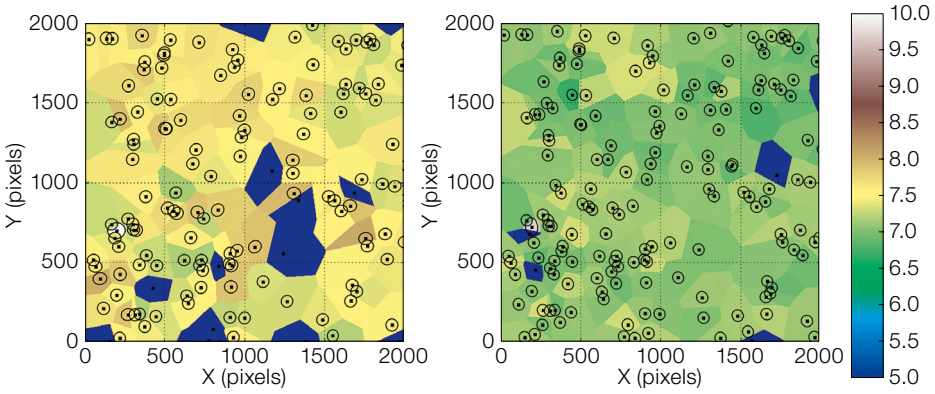

Figure 5. Images of the behaviour of the FWHM across HAWK-I images in *Y*-band at airmass 1.0. Left: with the Dornier M2 unit; Right: with the DSM. The scale shows the FWHM in pixels (pixel scale is 0.106 arcseconds) and annuli around the star positions indicate measured ellipticity.

First commissioning of the GALACSI Wide Field Mode

On 12 March 2017, following re-integration and verification in the NIH, the GALACSI module (La Penna et al., 2014; Arsenault et al., 2013b; Stuik et al., 2012) was transported to UT4 and installed on the Nasmyth platform (Figure 7). Precautions were taken to protect the MUSE hardware during installation (a special protective fence was designed and manufactured). First light was obtained on 20 March on GALACSI, despite an emergency telescope shutdown which delayed the GALACSI installation by one week.

In April 2017, there was another on-sky commissioning run during which many technical tests were conducted to reliably enable the full adaptive optics correction performance of the GALACSI WFM, making use of the DSM and the 4LGSF (Hackenberg et al., 2014; Bonaccini Calia et al., 2014; Holzlöhner et al., 2008; Holzlöhner et al., 2010; Holzlöhner et al., 2012; Amico et al., 2015). The complete automatic acquisition sequence was run on numerous occasions and timed. The acquisition involves presetting the telescope to the target, acquiring the 4 Laser Guide Stars within the 5 arcsecond field

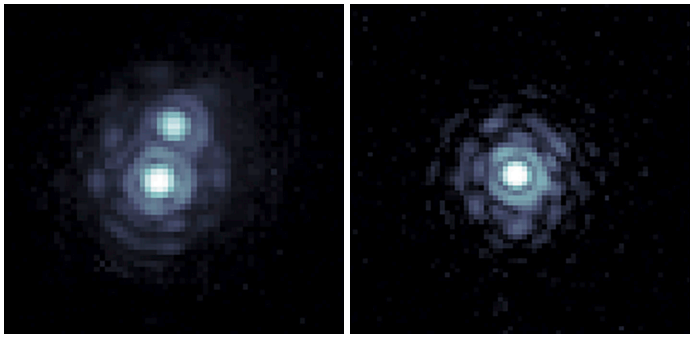

Figure 6. Left: *K*-band narrow filter image of a double star with 0.2 arcsecond separation, obtained with GRAAL MCM. Right: A bright star image exhibiting 80 % Strehl ratio (also with *K*-band narrow filter). The seeing was 0.55 arcseconds at the time.

Figure 7. Left: GALACSI being hoisted through the azimuth hatch after transport from the Paranal New Integration Hall to UT4. Right: The very tight margin to manoeuver this sensitive module between the Nasmyth acquisition and image rotator unit and the MUSE fore-optics can be seen.

of view of the four GALACSI wavefront sensors, performing the detection and centering of the tip-tilt natural guide star, and then closing all the loops. The final results are impressive; after a few nights spent on improving the automatisation of this process, the overhead for the AOF acquisition after the telescope is ready (two active optics cycles) was measured to be less than one minute (50 seconds). It should be remembered that the specification for the overhead was 5 minutes and the goal 2 minutes.

Amongst many performance tests conducted, one of them consisted of evaluating the stability of the registration between the actuator pattern of the DSM and the WFS sub-aperture pattern. Shifts with respect to one another are due to mechanical flexure in the large distance between them and could lead to a degradation of the optical quality of the images delivered by GALACSI to MUSE. Figure 8 shows that, thanks to a rigid design and good optical alignment, the stability of the pupil shift is pretty good from zenith down to 35° altitude, meaning that a compensation strategy for this misalignment may not be needed, thus simplifying the GALACSI operations.

Rejection transfer functions have been measured for both the high-order correction loop and the tip-tilt loop. Both look good and can be fitted nicely by the model of the dynamic system with respectively 1.3 ms and 4.3 ms of pure delay.

System performance has been finally characterised. A gain of 1.5–2 in FWHM at 750 nm was observed between open loop (with telescope field stabilisation) and full closed loop. The seeing matched the atmospheric specification (~1.1 arcseconds) and the target was low in the sky (zenith distance 50°). This is a very good first sign that the GALACSI WFM performs as specified. The ratio of turbulence in the first 500 metres above the telescope to the total turbulence given by the SLOpe Detection And Ranging (SLODAR) measurement and the internal estimation was ~90 % — i.e., quite high — a situation which is best suited to ground-layer AO correction (Kuntschner et al., 2012). Figure 9 illustrates this correction but much better results were obtained later.

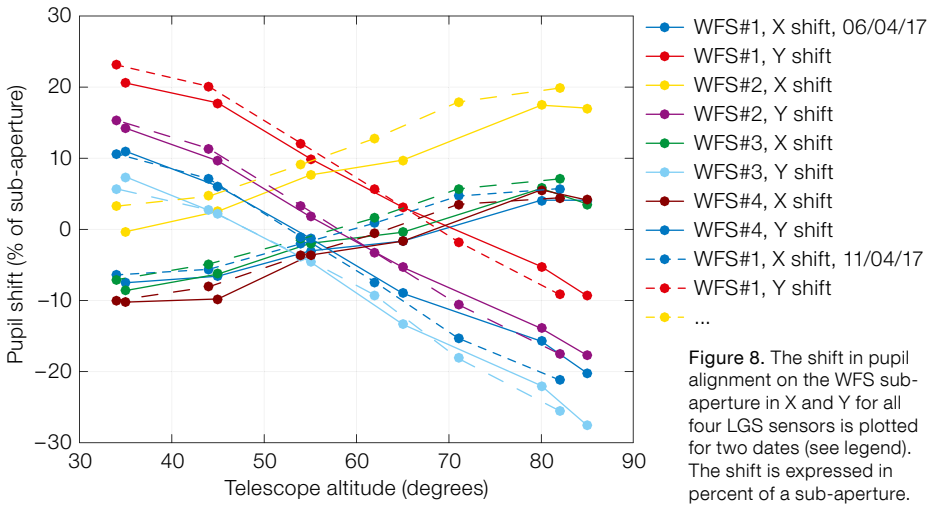

Figure 8. The shift in pupil alignment on the WFS sub-aperture in X and Y for all four LGS sensors is plotted for two dates (see legend). The shift is expressed in percent of a sub-aperture.

The results obtained during later nights improved somewhat, and the statistics showed much better performance. The gain between GLAO and non-GLAO depends strongly on the fraction of turbulence in the lower atmospheric layers. If a large fraction is concentrated below 500 metres, GALACSI will substantially improve the ensquared energy (a gain of four has been obtained). Conversely, if this fraction falls below ~20 %, the gain will be lower and the observer must decide whether seeing-limited observations must be conducted (with shorter acquisition time and without lasers) or simply another mode (MUSE NFM) or instrument. This information is provided from Multi-Aperture Scintillation Sensor (MASS) and Differential Image Motion Monitor (DIMM) data at the Observatory. Figures 10 and 11 demonstrate the ensquared energy performance with open and closed loop, allowing a first assessment of gains, but with limited statistics. From Figure 11, one can determine that

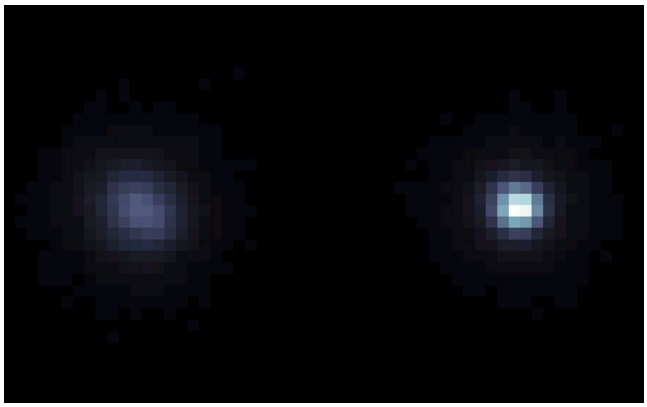

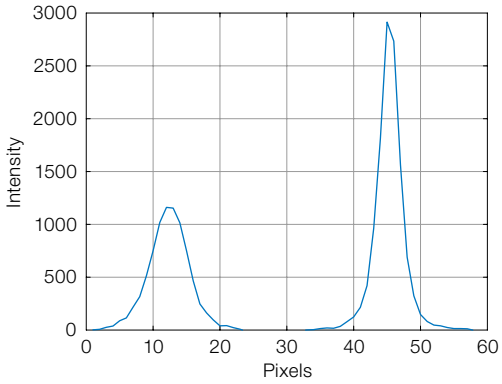

Figure 9. The quality of the image enhancement by GLAO correction is illustrated by before and after images (left) and profiles through the image centres (right). See text for full description.

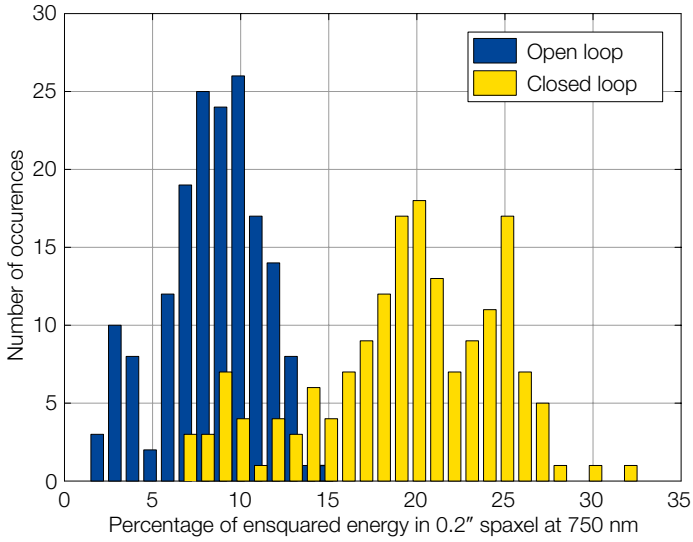

Figure 10. The distribution of values of ensquared energy per 0.2 arcsecond spaxel with GLAO loop is shown for closed loop (yellow) and open loop (blue; only with field stabilisation).

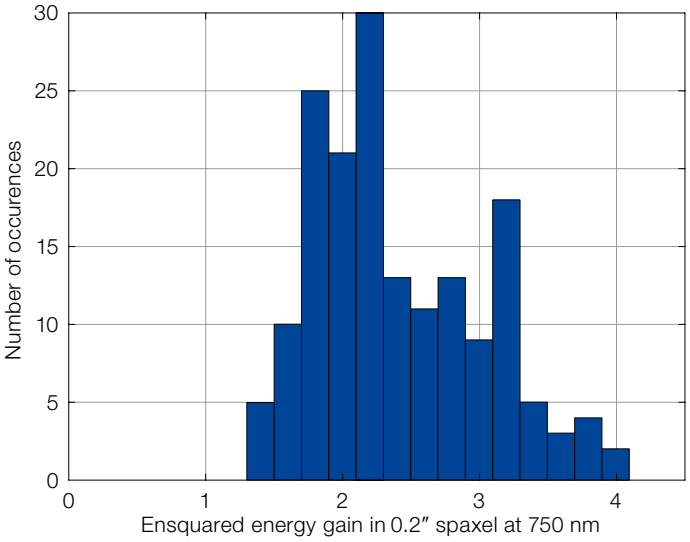

Figure 11. The distribution of gain in ensquared energy per 0.2 arcsecond spaxel with GLAO loop correction is plotted.

a gain of 2.0 can be obtained about 69 % of the time, a gain of 1.9 76 % of the time and a gain of 1.8 83 % of the time. We will closely follow up how these histograms evolve as more statistics are collected with successive commissioning runs.

During one of the commissioning nights, the patch of sky where we pointed happened to have a nice target in the middle, so we couldn't resist taking images at 850 nm with the commissioning camera (Figure 12). The left-hand image of Saturn was taken with field stabilisation; the right hand image with full GLAO. The seeing was fair (0.8 arcseconds) and the pointing was almost at zenith for these observations.

Finally, we could verify that the sensitivity of GALACSI was consistent with that measured on ASSIST in Garching. The tests were performed on an 18.6 magnitude star, the loop was closed and was stable, and the performance was within specification (the specified limiting magnitude of GALACSI is 17.5). Figure 13 shows the raw image on which the loop is closed (left), and the resulting images from averages of 50 frames (centre) and 12 000 frames (right). The 50-frames average will be shown in the GALACSI display panel, so that the user can be confident that the loop is locked on a star.

Conclusions: AOF is on-sky!

Since March 2017, the AOF has been fully installed on UT4. The 4LGSF was the first AOF component to be bolted onto the telescope and it is fully commissioned on-sky (first light was in April 2016). Then the new M2 unit (DSM) was installed and replaced the old Dornier M2 unit in October; since then, the new M2 unit is routinely being used by the TIOs to make science observations with the suite of UT4 instruments. GRAAL was attached to the telescope in late 2016, but will not be fully commissioned until the end of 2017. Last but not least, GALACSI is now also available at Paranal. GALACSI WFM commissioning has begun and the

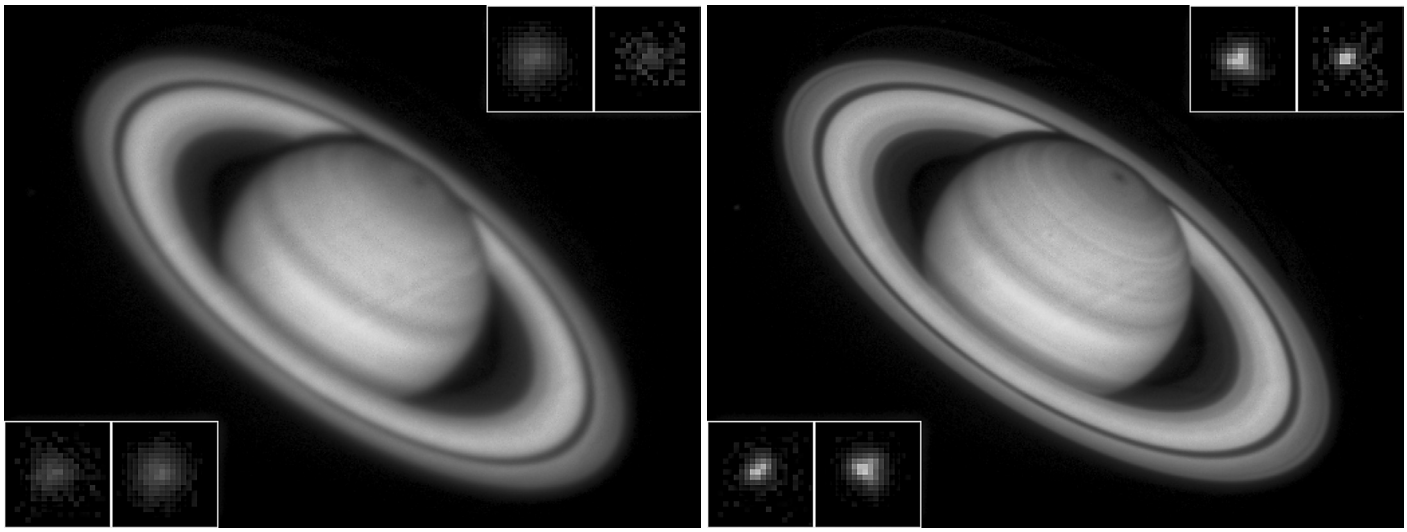

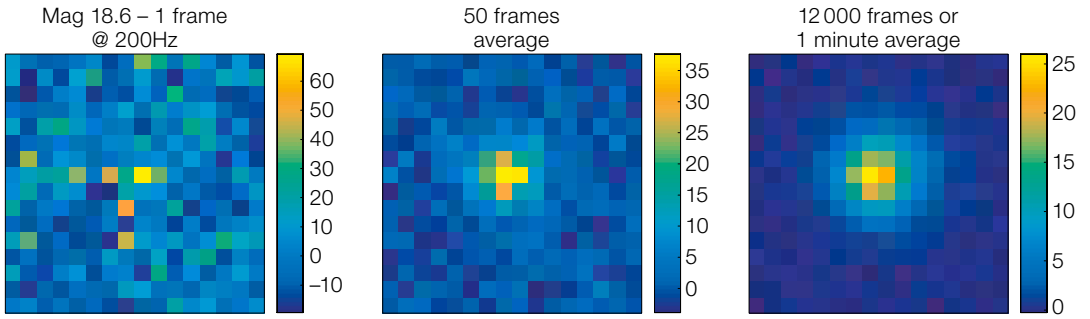

Figure 12. (Above) Saturn observed without (left) and with (right) GLAO. The insets show the effect of the correction on some stellar images.

Figure 13. Individual 200 Hz frame showing the tip-tilt star signal (left), with 50 (centre) and 12 000 (right) frames averaged. The star magnitude is 18.6 and the spaxel size is 0.2 arcseconds.

performance is found to be extremely promising so far.

As an anecdote, the AOF team took the picture shown in Figure 14, illustrating better than a long speech and without ambiguity that the AOF is now on sky (for readers interested in the technical details, each character is created using one laser guide star by controlling its associated 1 kHz jitter mirror; the image was recorded during a 4 s exposure of the Laser Pointing Camera installed on the telescope top ring).

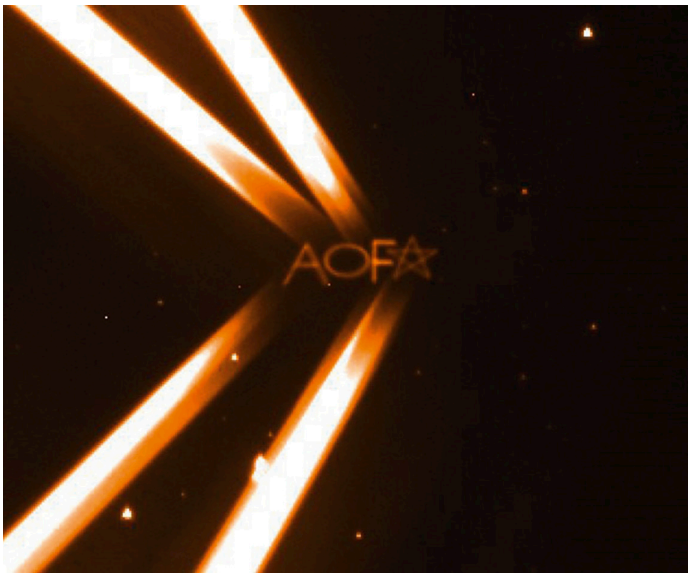

Figure 14. The writing is on … the sky!

References

Amico, P. et al. 2015, The Messenger, 162, 19
Arsenault, R. et al. 2010, The Messenger, 142, 12
Arsenault, R. et al. 2013a, The Messenger, 151, 14
Arsenault, R. et al. 2013b, Third AO4ELT Conference, Florence, Italy
Arsenault, R. et al. 2014a, Proc. SPIE, 9148, 914802
Arsenault, R. et al. 2014b, The Messenger, 156, 2
Arsenault, R. et al. 2016, The Messenger, 164, 2
Bonaccini Calia, D. et al. 2014, Proc. SPIE, 9148, 91483P
Briguglio, R. et al. 2014, Proc. SPIE, 9148, 914845
Hackenberg, W. et al. 2014, Proc. SPIE, 9148, 91483O
Holzlöhner, R. et al. 2008, Proc. SPIE, 7015, 701521
Holzlöhner, R. et al. 2010, A&A, 510, A20
Holzlöhner, R. et al. 2012, Proc. SPIE, 8447, 84470H
Kuntschner, H. et al. 2012, Proc. SPIE, 8448, 844808
La Penna, P. et al. 2014, Proc. SPIE, 9148, 91482V
Manetti, M. et al. 2014, Proc. SPIE, 9148, 91484G
Paufique, J. et al. 2012, Proc. SPIE, 8447, 944738
Stuik, R. et al. 2012, Proc. SPIE, 8447, 84473L